

# Zero Mean Noise Processes that Do Not Appear to be Zero Mean

Victor S. Reinhardt, *Raytheon Space and Airborne Systems*

## BIOGRAPHY

Victor S. Reinhardt received his Ph.D. and M.A. from Harvard University and his B.A. from New York University, all in physics. He is currently employed at Raytheon Space and Airborne Systems as an Engineering Fellow and prior to that worked at Boeing Satellite Systems (previously Hughes Space and Communications) where he retired as a Chief Scientist and Technical Fellow. Before this, he was lead for the NASA GSFC precise time and frequency standards program. His technical activities include both systems analysis and detailed hardware and software design in the areas of frequency synthesis, communications, radar, navigation, and geodesy. He is a member of the IEEE, ION, and APS and has authored 23 patents and 50 papers. He also serves on various advisory and standards committees for the IEEE and ITU.

## ABSTRACT

This paper shows that correlated but random zero mean noise processes can cause estimation filters (such as Kalman and least squares filters) to generate anomalous results that are similar to those generated by unmodeled non-zero mean causal behavior. The paper discusses two types of such noise processes: stationary Poisson and Gauss-Markov processes and non-stationary negative power law (neg-p) processes. The paper shows that such anomalous results are due to two factors. First, it is shown that single ensemble members of such correlated noise processes exhibit non-ergodic-like behavior over a finite data collection interval  $T$ , if  $\tau_c$  the correlation time of the noise process is an appreciable fraction of  $T$ , even if the process is strictly ergodic as  $T \rightarrow \infty$ . This these causes practical realizations of such filters, which rely on ergodic-like behavior in a single ensemble member for their proper operation, to generate results that deviate from theoretically predicted behavior. Second, it is shown that the signatures over  $T$  of such individual ensemble members can mimic those of the desired signal being estimated. This causes the filter to treat such noise as part of the desired signal and leads to the underestimation of the true error generated by the noise. It is then shown that setting  $T \gg \tau_c$  allows one to properly separate the noise from the desired signal and to properly estimate the true error. It is further shown that  $\tau_c \rightarrow \infty$  for neg-p noise, and

thus one can never separate the correlated part of such noise from the desired signal, regardless of the value of  $T$ . This is shown to lead to infinite true errors for neg-p noise unless one introduces periodic calibration to bound the divergent effects of such noise. The paper concludes with a description of (causal) environmentally induced errors that mask their causal nature and exhibit behavior similar to correlated ZM noise processes.

## INTRODUCTION

Estimation filters, such as Kalman [1] and least squares [2] filters, are used to extract estimates of causal behavior from noisy data. Sometimes these filters generate results that seem to be in conflict with theoretically expected behavior. Generally, this anomalous behavior is attributed to the presence of an unmodeled causal or non-zero mean process in the data. However, this is not always the case. In this paper, we will show that such anomalous behavior can be generated by a random zero mean (ZM) noise process, if the process in question is correlated from sample-to-sample. We will also discuss in detail how two classes of correlated noise processes cause such anomalous behavior: stationary Poisson and Gauss-Markov processes and non-stationary negative power law (neg-p) processes. We will conclude our discussion with a description of (causal) environmentally induced errors that mask their causal nature and exhibit behavior similar to correlated ZM noise processes.

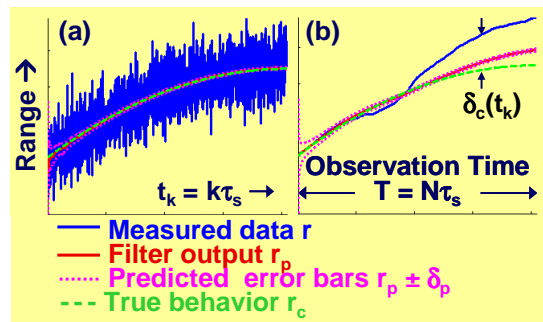


Figure 1. (a) Expected and (b) unexpected behavior in a Kalman estimation filter.

As an example of such anomalous behavior, consider Figure 1. This figure shows both: (a) theoretically expected and (b) unexpected results generated by a Kalman filter. Here, a simple Kalman filter model (which

will be used throughout this paper) is used. This model generates an estimated range output from one-dimensional ranging data containing noise. The model is defined as follows. First, the basic parameters in the model are given by

- $r(t_k) = r_c(t_k) + x(t_k)$  is measured ranging data.
- $t_k = t_0 + k\tau_s$  is the sampling time ( $k = 0$  to  $N-1$ ).
- $\tau_s$  is the sampling interval.
- $T = N\tau_s$  the data observation or collection interval.
- $r_c(t_k)$  is the true range.
- $x(t_k)$  is the measurement error.
- $r_p(t_k)$  is the filter estimated range output.
- $\delta_p(t_k)$  is the predicted error generated from the filter covariance output.
- $\delta_c(t_k) = r_p(t_k) - r_c(t_k)$  is the true error.
- The subscript  $k$  will often be dropped for simplicity or to indicate the continuous process.

Second, the differential state model [1,3] is given (in Matlab matrix notation) by

$$\begin{aligned} \underline{s}(t_k + \tau_s) &= \underline{A}(t_k + \tau_s, t_k) \cdot \underline{s}(t_k) + \underline{u}(t_k) + \underline{w}(t_k) \\ r(t_k) &= \underline{H}(t_k) \cdot \underline{s}(t_k) + x(t_k) \end{aligned} \quad (1)$$

- The underscore indicates a vector or matrix.
- $\underline{A}(t_k + \tau, t_k) = [1 \ \tau_s; 0 \ 1]$  is the state transition matrix.
- $\underline{u}(t_k) = [0; -\tau_s]$  is the casual forcing function.
- $\underline{w}(t_k) = [0; 0]$  is the process noise vector.
- $\underline{s}(t_k) = [r(t_k); dr(t_k)/dt]$  is the state vector.
- $dr(t_k)/dt$  is the measured range rate.
- $\underline{H}(t_k) = [1; 0]$  is the observation matrix.

In Figure 1(a), where the noise is uncorrelated (white) from sample-to-sample, note that  $r_p(t_k)$  is consistent with  $r_c(t_k)$  and that  $\delta_p(t_k)$  is consistent with  $\delta_c(t_k)$ . In Figure 1(b), on the other hand, the filter behavior is very different. Here, it looks like  $x(t_k)$  contains some unmodeled non-zero mean behavior that causes  $r(t_k)$  to systematically deviate from  $r_c(t_k)$  and  $\delta_p(t_k)$  to be inconsistent with  $\delta_c(t_k)$ . Figure 1(b), however, was generated by purely random ZM noise that is correlated from sample-to-sample.

We note that we will be talking about measurement noise  $x(t_k)$ , which is represents the difference the measured and true behavior  $r_c(t_k)$ , not process noise  $\underline{w}(t_k)$ , which is a proper part of  $r_c(t_k)$ , even if it is random. Thus, our model sets  $\underline{w}(t_k)$  to zero as a non-essential simplification. We finally note that our over-all conclusions will not be dependent on the details of our simple illustrative model. They will be based on very general principles that apply to virtually any type of model and estimation filter.

## WHAT IS MEANT BY A ZERO MEAN (ZM) RANDOM PROCESS?

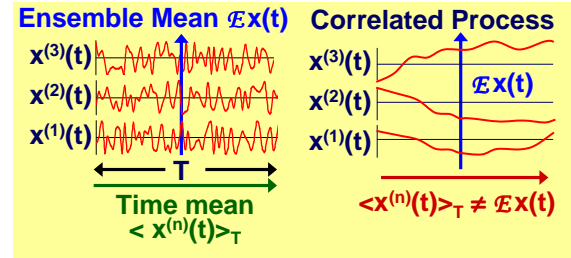


Figure 2. Ensemble and time means.

To understand how a ZM process can exhibit the behavior shown in Figure 1(b), one must understand what the term ZM implies and does not imply. Formally, a ZM process is one where  $E\{x(t)\} = 0$ , that is, where the ensemble average  $E$  of  $x(t)$  at any  $t$  is zero [2,4,5,6]. This shown in Figure 2. Here, we note that  $E\{x(t)\}$  designates the average over different ensemble members  $x^{(1)}(t)$ ,  $x^{(2)}(t)$ , ... at a each  $t$ . It is important to note that ensemble averages are used to generate the theoretical equations that define a statistically optimum estimation filter [1,2,4,5].

In Figure 2, we also note other type of average that is used in generating practical realizations of an estimation filter. This is  $\langle x^{(n)}(t) \rangle_T$  the time average of a single ensemble member  $x^{(n)}(t)$  over a finite data collection interval  $T$ . It is important to note that this difference in averaging between the theoretical filter and its practical realization is not often stated, but is always implicit, because one only operates on a single ensemble member in a practical realization.

A mean ergodic process is one where [4,6]

$$E\{x(t)\} = \lim_{T \rightarrow \infty} \langle x(t) \rangle_T \quad [\text{mean ergodic}] \quad (2)$$

Note, this implies that  $E\{x(t)\}$  is not a function of  $t$ , because the limiting process takes out all time references [5,6]. Further, note (see Figure 2) that ergodicity does not imply that  $E\{x(t)\} = \langle x^{(n)}(t) \rangle_T$  or that  $\langle x^{(n)}(t) \rangle_T$  is independent of the time for finite  $T$ , especially when the process is correlated.

The theoretical (ensemble averaged) covariance of a non-stationary (NS) noise process  $x(t)$  is given by [7]

$$C_x(t_g, \tau) = E\{x(t_g + 0.5\tau)x(t_g - 0.5\tau)\} \quad [\text{NS}] \quad (3)$$

Here, we are explicitly assuming that: (a)  $E\{x(t)\} = 0$  is zero so the covariance and correlation function [4] are the same, and (2) we are using the “rotated” time arguments  $t_g$  the global time from the start of the noise process and  $\tau$

the difference or local time [7]. Note that the theoretical variance of  $x(t)$  is given by

$$\sigma_x^2(t_g) = C_x(t_g, 0) \quad (4)$$

If the process is wide-sense stationary (WSS), then  $C_x(t_g, \tau)$  is time translation invariant and thus only a function of  $\tau$  [4,6]; that is

$$C_x(\tau) = \mathcal{E} x(t_g + 0.5\tau)x(t_g - 0.5\tau) \quad [\text{WSS}] \quad (5)$$

In this case,  $\sigma_x^2$  must be independent of  $t$  [4,6]. It is important to note that a process cannot be truly WSS unless  $x(t)$  is statistically bounded in some sense (which implies that  $\sigma_x^2$  is bounded) [2,8]. This is often not explicitly stated in the definition of an WSS process. However, many theorems about WSS processes break down if this assumption is violated [2,8]. An important theorem connecting NS and WSS processes is [9,10]

$$C_x(\tau) = \lim_{t_g \rightarrow \infty} C_x(t_g, \tau) \quad (6)$$

Thus, a process cannot be WSS if  $C_x(t_g, \tau) \rightarrow \infty$  as  $t_g \rightarrow \infty$ .

One can define a covariance ergodic process by substituting the covariance for the mean in the above discussion [4]. Here, the finite time averaged equivalent of  $\langle x^{(n)}(t) \rangle_T$  is

$$C_x^{(n)}(t_g, \tau, T) = \langle x(t_g + 0.5\tau)x(t_g - 0.5\tau) \rangle_T \quad (7)$$

For covariance ergodicity, one therefore must have

$$C_x(\tau) = \lim_{T \rightarrow \infty} C_x^{(n)}(t_g, \tau, T) \quad [\text{covariance ergodic}] \quad (8)$$

We note that  $x(t)$  must be WSS if it is covariance ergodic because  $T \rightarrow \infty$  takes out references to a finite starting point.

### THE CONNECTION BETWEEN ANOMALOUS AND NON-ERGODIC-LIKE BEHAVIOR

What does the above discussion of ergodicity have to do with noise-generated anomalous behavior in estimation filters? The answer relates to the replacement of the ensemble average in the theoretical filter by the finite time average over one ensemble member in the practical realization of the filter. Thus, for the practical realization to act like its theoretical counterpart, these finite time averages must approximately reproduce the behavior of ensemble averages. We will call this ergodic-like

behavior. As one can see in Figure 2, this can happen, even if the noise process is strictly ergodic as  $T \rightarrow \infty$ .

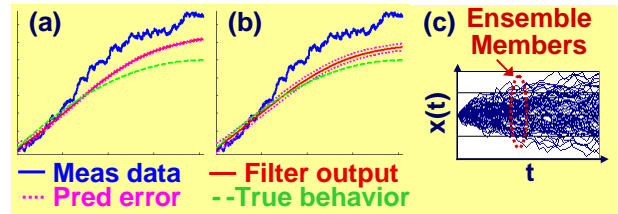


**Figure 3. Kalman solutions with random walk  $x(t_k)$ . (a) is the basic Kalman model. In (b), the Kalman model is augmented with a correlated noise model. (c) shows the NS and non-ergodic-like nature of random walk noise.**

This connection between anomalous filter behavior and non-ergodicity is demonstrated in Figure 3. Figure 3(a) shows our Kalman filter model generated using a single ensemble member of a ZM random walk  $x(t)$  process shown in Figure 3(c) [9]. Here, one can clearly see the anomalous filter behavior caused by the random walk. In Figure 3(c), we have generated multiple ensemble members to emphasize the non-ergodic-like behavior of single ensemble members.

Figure 3(b) demonstrates a second important principal that causes anomalous Kalman filter behavior. Here, the filter is augmented [1] by a correlated random walk  $x(t)$  model [9] that is supposed to correct for the correlated noise process. Note that the filter does a somewhat better job of predicting the true behavior and of estimating the true errors but that the results are far from perfect. The question of what is happening here is answered by drawing on another important principal in estimation theory, the Orthogonality Principal [1,4,5]. The Orthogonality Principle states that the residual error from the estimated output in a minimum mean square (MMS) estimation filter must be orthogonal to the filter output in an appropriate Hilbert space [1,4,5]. In other words, an estimation filter cannot properly separate  $x^{(n)}(t)$  from  $r_c(t)$  to the extent that  $x^{(n)}(t)$  is linearly dependent with  $r_c(t)$  over  $T$ . This principal also applies to more general solution techniques. It is just a specific application of the fact that solution equations become ill-formed when the determinant of the solution matrix is near zero [11]. It is also well known in least squares fit (LSQF) theory as the fact that a LSQF solution cannot separate errors that are systematic with the causal behavioral model over  $T$  [5]. Therefore,  $r_p(t)$  must follow the parts of  $x^{(n)}(t)$  that are systematic with  $r_c(t)$ , and also underestimates the true error, because the filter treats the systematic part of  $x^{(n)}(t)$  as if it were true behavior.

## STATIONARY EXEAMPLES OF CORRELATED NOISE

A Poisson or random telegraph process and a Gauss-Markov processes are simple examples of correlated but ZM noise processes that can generate anomalous behavior in estimation filters. A Poisson process is a strict-sense stationary [4] ergodic process whose random variable changes state with a Poisson probability at some average rate given by  $1/\tau_c$  [4,6]. This process can be non-ZM or ZM depending on the value of  $\mathcal{E}x(t)$ . A Gauss-Markov process is a similar-strict sense stationary ergodic process generated by the single pole lowpass filtering of white noise [4]. Both have the same WSS autocovariance given by [4]

$$C_x(\tau) = \sigma^2 \exp(-|\tau|/\tau_c) \quad (9)$$

$\tau_c$  is also the correlation time for these processes defined as [12]

$$\tau_c = 0.5C_x(0)^{-1} \int_{-\infty}^{+\infty} d\tau C_x(\tau) \quad (10)$$

$\tau_c$  is heuristically the time range over which  $x^{(n)}(t+\Delta t)$  is appreciably dependent on the particular value of  $x^{(n)}(t)$  that occurred. Such correlated noise processes are typically generated by random-like environmental changes as well as under sampling for the Nyquist bandwidth of the system.

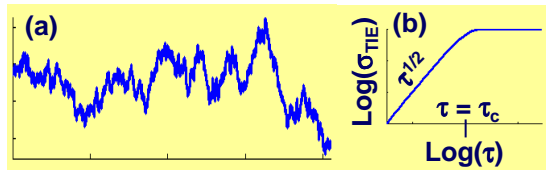


Figure 4. Gauss-Markov process.

The time behavior of a Gauss-Markov process is shown in Figure 4(a) (a Poisson process has similar though more stepped behavior). Figure 4(b) shows that such processes behave like random walks for time intervals  $\tau$  less than  $\tau_c$ . Here, we've plotted  $\sigma_{TIE}$  the RMS of the 1st difference of  $x(t)$  over  $\tau$  given by [13]

$$\sigma_{TIE}^2(\tau) = \mathcal{E} [x(t + \tau) - x(t)]^2 \quad (11)$$

This is well-known as the RMS Time Interval Error (TIE) when  $x(t)$  is the time error [13,14]. One can see that  $\sigma_{TIE}$  increases as  $\tau^{1/2}$  for  $\tau < \tau_c$  for such noise, and this  $\tau^{1/2}$  behavior is a defining characteristic of random walk noise [4,9]. Thus, one would expect Kalman filter results for Poisson and Gauss-Markov processes to be similar to that of the random walk results shown in Figure 3 when  $\tau_c$  is on the order of  $T$  or greater.

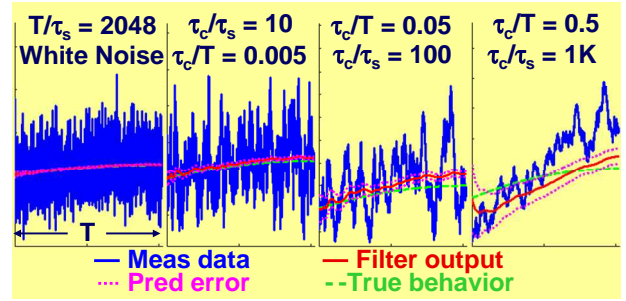


Figure 5. Effect of  $\tau_c$  on Kalman filter results for a Gauss-Markov process.

Figure 5 shows this is indeed the case. Here, Kalman filter results are shown as a function of  $\tau_c$ . (No augmentation of the filter is used here.) When  $\tau_c > \tau_s$  ( $\tau_s$  is the sample interval), one can see that the predicted behavior starts to become anomalous. This is due to the well-known reduction in the number of degrees of freedom from the number of samples  $N = T/\tau_s$  to  $N_c = T/\tau_c$  for correlated noise [12]. As  $\tau_c$  approaches the value of  $T$ , we note that the filter output deviates more and more from the true behavior until the filter output severely misrepresents the true behavior.

It is well-known that one can correct such misrepresentations for any stationary correlated noise process simply by making  $T \gg \tau_c$ , regardless of the value of  $\tau_c/\tau_s$ . The only proviso is that  $N_c$  must be used in calculating errors, rather than  $N$ . For neg-p processes, this is not the case, as is explained in the section that follows.

## NEGATIVE POWER LAW (NEG-P) NOISE

The random walk noise we've previously discussed is an example of negative power law (neg-p) noise. These are noise processes that are well-known in time and frequency sources, and get their neg-p name from their  $S_p(f) \propto f^p$  (for  $p < 0$ ) power spectral densities (PSDs) [9,14]. The well known types of integer neg-p noise when  $x(t)$  is the time or phase error are listed in Table I.

| Name ( $S_p(f) \propto f^p$ ) | $p$ |
|-------------------------------|-----|
| Flicker of phase              | -1  |
| Random walk of phase          | -2  |
| Flicker of frequency          | -3  |
| Random walk of frequency      | -4  |

Table I. Well-known types of integer neg-p noise when  $x(t)$  is the time or phase error.

Neg-p noise, however, is actually NS, so it cannot strictly be represented by a WSS PSD [9], despite the fact that such PSDs are generally used for analyzing neg-p noise [14]. For integer neg-p noise, one can show that such noise has the following (nasty) properties [9]

- $C_x(t_g, \tau)$  is bounded for all  $t_g$  and  $\tau$ , but becomes infinite for  $t_g \rightarrow \infty$  [9].
- $x(t)$  never reaches a statistical steady state ( $x(t)$  unbounded as  $t_g \rightarrow \infty$ ).
- $C_x(\tau)$  is strictly infinite for all  $\tau$ . Thus one cannot strictly use the WSS representation in the time domain. (An exception will be given later.)
- $\tau_c \rightarrow \infty$  as  $t_g \rightarrow \infty$  and  $\tau_c$  is on the order of the maximum  $t$  in the problem for finite  $t_g$ .
- Thus,  $\tau_c$  is at least on the order of  $T$  and thus one can never have a situation where  $T \gg \tau_c$ .

One can simulate integer neg-p noise by Wiener filtering white noise [4,9]. In the NS representation, such Wiener filtering is written as [9]

$$x_p(t) = \int_0^t d\tau h_p(t-\tau)x_0(\tau) \quad (11)$$

where  $x_0(t)$  indicates white noise ( $p=0$ ) and  $x_p(t)$  indicates power law noise of order  $p$ . Formulas for such  $h_p(t)$  have been published [9,10,15,16] and they produce the simulated outputs shown in Figure 6.

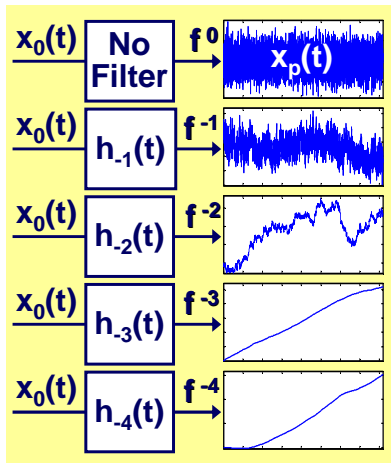


Figure 6. Wiener filter simulations of neg-p noise.

In the WSS representation, the Wiener filter convolution is given by [4,9]

$$x_p(t) = \int_{-\infty}^t d\tau h_p(t-\tau)x_p(\tau) \quad (12)$$

Thus, one can see  $x_p(t)$  is unbounded in the WSS representation for any  $t$ , because  $h_p(t)$  has an infinite memory ( $\tau_c = \infty$ ) [9]. In systems where  $x(t)$  contains additional system highpass (HP) filtering of  $x_p(t)$  given by  $H_s(f)$  (so that the filtered PSD is  $S_x(f) = |H_s(f)|^2 S_p(f)$  [4]), one can fix this divergence problem when the HP filtering of  $H_s(f)$  is sufficient to suppress the divergence of  $S_p(0)$  [17,18]. If such is the case, the filtered  $x(t)$  is a stationary

correlated ergodic process with a finite  $\tau_c$  determined by the properties of  $H_s(f)$  [17,18]. In this case, the WSS representation can be used to generate a finite filtered  $x(t)$  from the frequency domain  $S_x(f)$ . Thus, in this case, the previous discussion about stationary correlated processes applies.

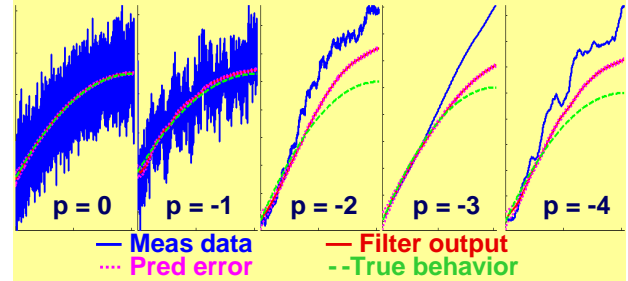


Figure 7. Kalman behavior for neg-p noise.

Figure 7 shows the effects of various integer orders of neg-p noise on our Kalman filter model when no system HP filtering is present. Here,  $t_g$  is set to 0 at the start of the simulation. For  $p=-1$ , anomalous Kalman behavior just begins to become apparent, and the anomalous Kalman behavior becomes very apparent for  $p < -1$ . Finally, we note that the filter output will become progressively worse estimator as  $T$  gets larger. This is because  $\sigma_{TIE}^2(t_g)$  grows as  $\ln(Bt_g)$  for  $p=-1$  ( $B$  is the analog bandwidth) and  $t_g^{-p-1}$  for integer  $p < -1$  (when  $\tau=t_g$  and  $t=0$  in (11)) [9,15].

The simulations in Figure 7 also show a danger in dealing with neg-p noise. Here, we have set  $t_g$  to zero at the start of the simulation graphing period, as is common practice. Thus, the errors look larger than expected but possibly manageable. However, as we have just discussed, the RMS error from neg-p noise grows without bound as  $t_g \rightarrow \infty$ . Therefore, if the actual physical situation is such that  $t_g$  is large at the start of a data collection period, a simulation in which  $t_g$  is set to 0 at the start of the data collection interval will severely under-report the true error.

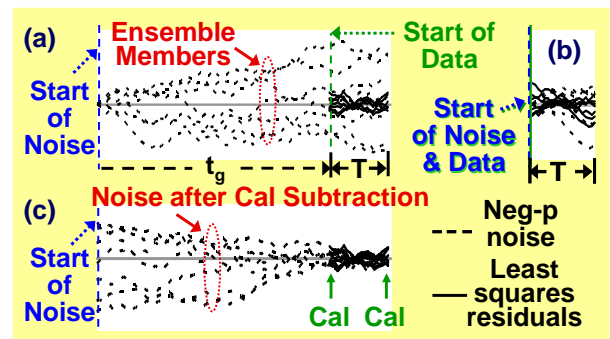


Figure 8. Effect of dependence on  $t_g$ .

This problem is illustrated in Figure 8 for random walk ( $p = -2$ ) noise. Here, results from a least squares fit (LSQF) are shown, where the LSQF in question predicts a constant offset (whose true value is zero) from noisy data over  $T$ . In the figure, we have plotted various ensemble members of the data (dotted lines) along with the residual fit error over  $T$  (solid lines). Here, these solid line residuals represent the apparent error due to the noise that one would infer from the LSQF and the dotted lines over  $T$  represent the true error. In Figure 8(b), where  $t_g$  is zero at the start of  $T$ , the true and apparent errors are comparable. However, Figure 8(a) represents the more physically realistic situation, where  $t_g$  is not zero at the start of the data collection period. One can see here that the differences between the true and apparent errors are much larger than in Figure 8(b), because of the accumulated error prior to the start of  $T$ .

This problem can of course be corrected when the system sufficiently HP filters  $x(t)$  by setting  $T \gg \tau_c$ . However, when there is no such system HP filtering, a different approach must be used. In Figure 8(c), we show such an approach. Here, we have introduced periodic calibration around  $T$  to remove accumulated errors. Thus, the true error during  $T$  remains small and comparable to the apparent error. This is effectively what the GPS system does for position location, because errors are periodically calibrated against known ground locations. We note, however, that this is not true for both the GPS and UTC timescales, since there is no absolute calibration available to remove time errors generated by accumulated atomic clock neg-p noise defining these time scales.

### ENVIRONMENT ERRORS THAT MASK THEIR ENVIRONMENTAL SIGNATURES

Environmental errors can be modeled and removed only if the functional relationships between measurement errors and environmental signatures can be identified. Hardware filtering can mask these functional relationships and make the true relationships hard to identify. The net result is errors that do not seem to correlate with environmental signatures and act like they are generated by correlated random noise. Figure 9 shows an example of such environmental behavior and its effect on our Kalman model. Here, we show the effect of ambient temperature slew rate ( $dK/dt$ ) sensitivity caused by such hardware filtering.

Such  $dK/dt$  sensitivity often occurs because many hardware components are differentially temperature compensated to a high degree. For example, the diodes in a double balanced mixer have typical diode drop voltage/temperature coefficients ( $dV/dK$ ) of about 1 mV/°C, while differential cancellation reduces the overall mixer AC signal zero crossing voltage/temperature coefficient to about 1  $\mu$ V/°C. When the temperature

slews, transient temperature gradients change across the diode bridge cause this differential cancellation to be temporarily unbalanced as a function of time. This produces a significant shift in the mixer AC signal zero crossing voltage proportional to  $dK/dt$  (which is often larger than the direct  $K$  sensitivity of the mixer). This in turn produces a phase shift in the output of the mixer proportional to  $dK/dt$  that can generate significant range measurement error in a navigation receiver.

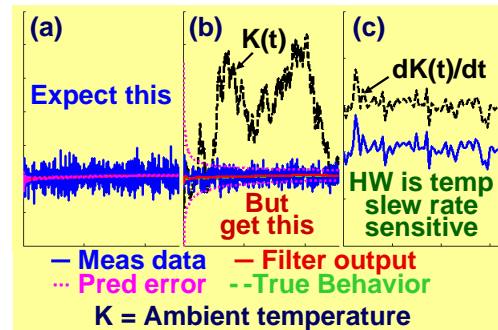


Figure 9. The effect of temperature slew rate sensitivity on a Kalman filter.

In Figure 9(a), Kalman filter output results are first shown when the input noise is white. Note the very small predicted errors relative to the measurement noise. Figure 9(b) shows the Kalman filter output with approximately the same level of measurement  $dK/dt$  “noise.” In Figure 9(b), note that the error bars are much wider than in Figure 9(a) and that the filter output and error bars seem to bear no relationship to the  $K(t)$  signature also shown in Figure 9(b). In Figure 9(c), a portion of the Figure 9(b) measured data is graphed along with  $dK(t)/dt$  to show the one-to-one match in behavioral signatures. The  $K(t)$  input here was generated using a correlated Gauss-Markov model differentiated in time. Typically, such correlations arise because hardware housings introduce thermal lowpass filtering and changes in the ambient temperature tend to be correlated.

### CONCLUSIONS

In this paper, we have shown that correlated but random zero mean noise processes can cause estimation filters to generate anomalous results similar to those normally associated with unmodeled non-zero mean behavior. We have shown that this arises due to the combination of two effects. First, a correlated noise process, even if it is stationary and ergodic over an infinite time, can exhibit non-ergodic-like behavior over a finite data collection interval. Second, such non-ergodic-like behavior can mimic the signature of the causal behavior being estimated, so the filter cannot distinguish this noise from the true behavior. These anomalous results can be reduced for stationary noise processes by making  $T$  the data collection interval greater than  $\tau_c$  the correlation time of the noise process. Neg-p noise is problematic in this area

because it has an infinite  $\tau_c$ , but periodic calibration can reduce the impact of this infinite  $\tau_c$ .

## REFERENCES

- [1] H. W. Sorenson, "Kalman Filtering Techniques," in *Advances in Control Systems* (Vol. 3), C. T. Leondes (Ed.), New York: Academic Press, 1966.
- [2] S. M. Kay, *Fundamentals of Statistical Signal Processing* (Vol. 1), Estimation Theory, Upper Saddle River, N. J.: Prentice Hall, 1993.
- [3] C. T. Chen, *Introduction to linear Systems Theory*, New York: Holt, Rinehart, and Winston, 1970.
- [4] A. Papoulis and S. U. Pillai, *Probability, Random Variables, and Stochastic Processes*, 4<sup>th</sup> ed., Boston MA: McGraw-Hill, 2002.
- [5] J. R. Wolberg, *Prediction Analysis*, Princeton, NJ: D. Van Nostrand and Co, 1967.
- [6] E. Parzen, *Stochastic Processes*, San Francisco, CA: Holden-Day, 1962.
- [7] L. L. Scharf, B. Firedlander, and D. J. Thomson, 1998, "Covavariant Estimators of Time-Frequency Descriptors for Nonstationary Random Processes," in *Proc. 32<sup>nd</sup> Asilomar Conference on Signals, Systems, and Computers, v1*, Pacific Grove, CA, 1998, pp 808-811.
- [8] W. B. Jr. Davenport and William L. Root, *An Introduction to the Theory of Random Signals and Noise*, New York, NY: McGraw-Hill, 1958.
- [9] V. S. Reinhardt, "Modeling Negative Power Law Noise," in *Proc. 2008 IEEE International Frequency Control Symposium*, pp. 685-592.
- [10] N.J. Kasdin and T. Walter, "Discrete Simulation of Power Law Noise", *Proc. 1992 IEEE Freq. Contrl. Symp.*, pp. 274-283, May 1992.
- [11] D. M. Young, *Iterative Solution of Large Linear Systems*, New York: Academic Press, 1971.
- [12] C. A. Greenhall, "Recipes for Degrees of Freedom of Frequency Stability Estimators," *IEEE Trans. I&M*, vol. 40, no. 6, Dec., 1991, pp. 994-99.
- [13] ITU-T G.810: ITU Definitions and Terminology for Synchronization Networks, International Telecommunications Union, 1996.
- [14] IEEE 1139-1999: Standard Definitions of Physical Quantities for Fundamental Frequency and Time Metrology—Random Instabilities, IEEE, 1999.
- [15] J. A. Barnes, "The Generation and Recognition of Flicker Noise," NBS Report 9284, NIST BIN: 190, June 12, 1967.
- [16] J. A. Barnes and S. Jarvis, Jr. *Efficient Numerical and Analog Modeling of Flicker Noise Processes*, NBS Tech. Note 604, U.S. Government Printing Office CODEN: NBTNA, NIST BIN: 29, June 1, 1971.
- [17] V. S. Reinhardt, "How Extracting Information from Data Highpass Filters its Additive Noise," in *Proc. 39th PTTI Systems and Applications Meeting, Dec., 2007*, pp. 559-580.
- [18] V. S. Reinhardt, "On Difference Variances as Residual Error Measures in Geolocation," in *Proc. Institute of Navigation 2008 National Technical Meeting, Jan., 2008*, pp. 763-772.